Figure S1. Phenotypic comparison betweenWT and *gsd1-D* mutant.

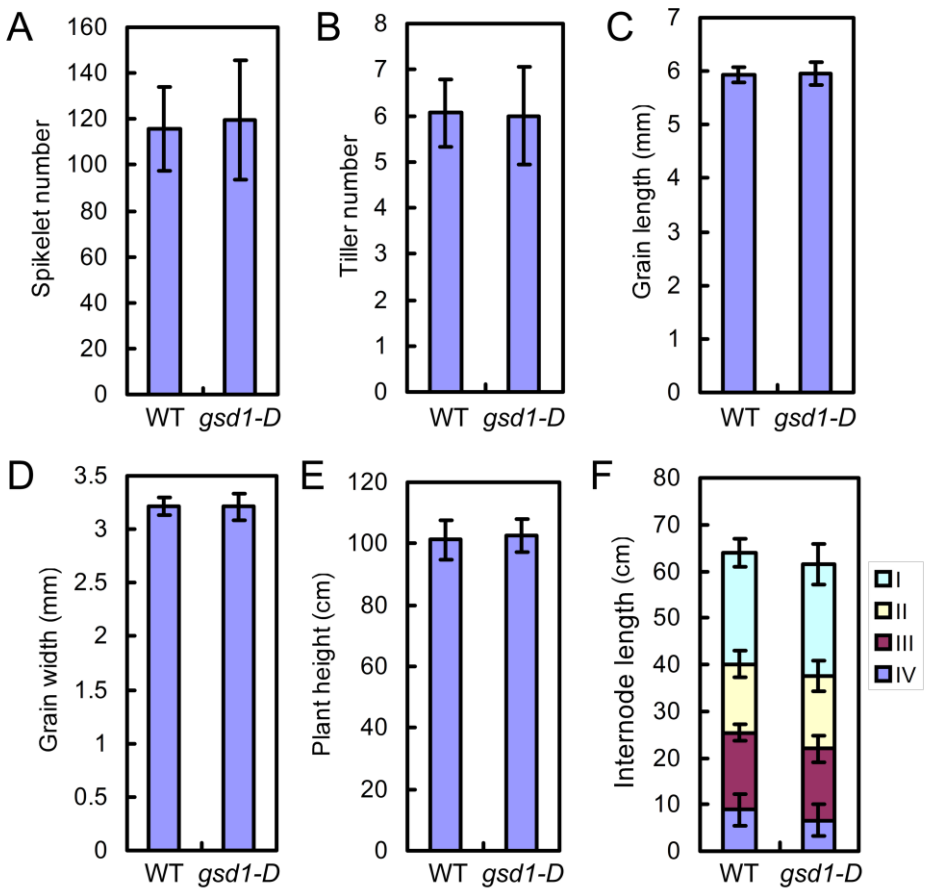

(A) The spikelet number per panicle between WT and *gsd1-D* mutant.

(B) The tiller number per plant between WT and *gsd1-D* mutant.

(C) The grain length between WT and *gsd1-D* mutant.

(D) The grain width between WT and *gsd1-D* mutant.

(E) The plant height between WT and *gsd1-D* mutant.

(F) The internode length between WT and *gsd1-D* mutant.

Figure S2. Microscopic analyses of rice flower morphology between wild-type and *gsd1-D* mutant at heading stage.

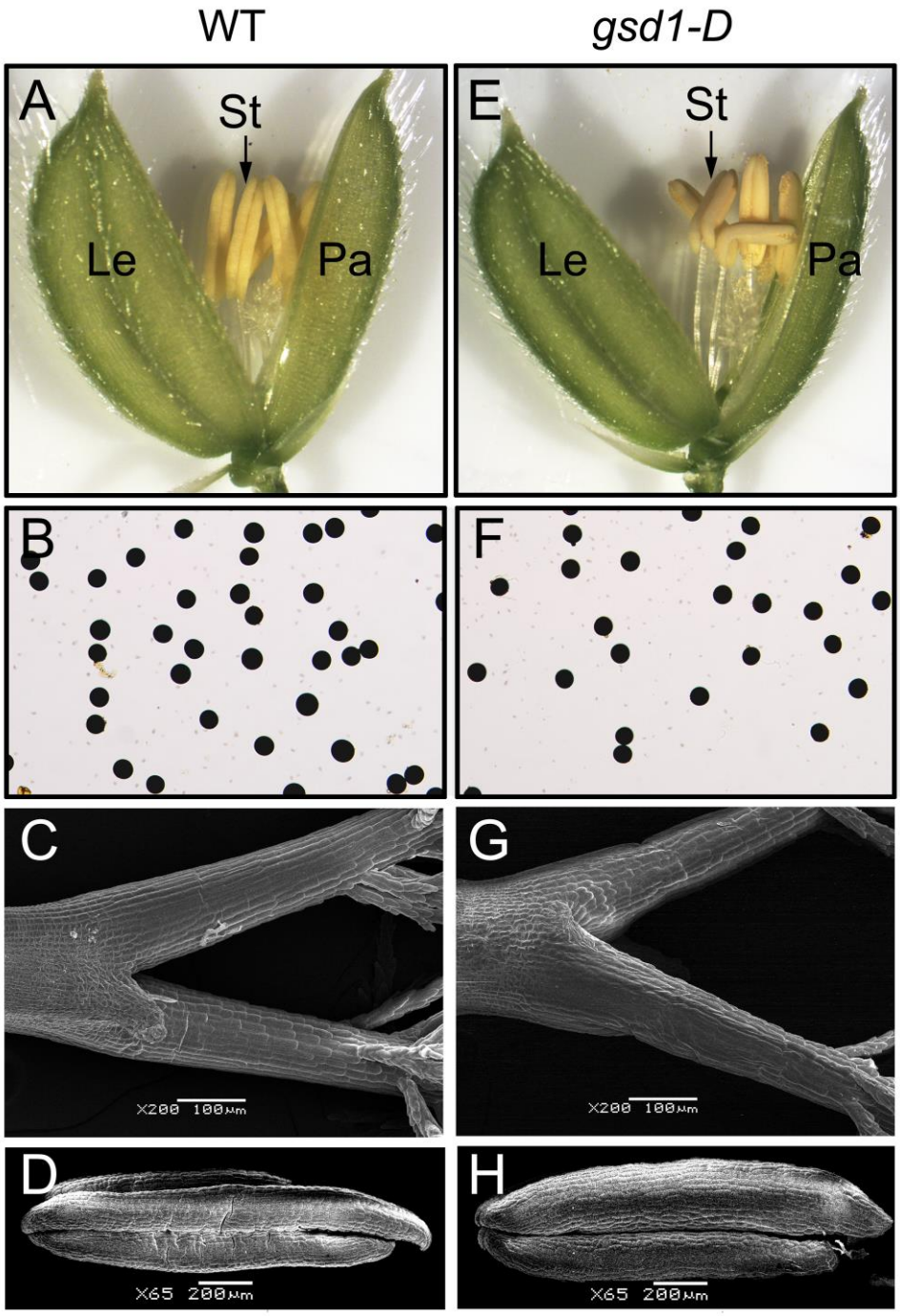

(A) and **(E)** Spikelet between WT (A) and *gsd1-D* mutant (E). Le, lemma; Pa, palea; St, stamen.
(B) and **(F)** I_2-KI staining of flowering pollen in WT (B) and *gsd1-D* (F).
(C) and **(G)** SEM observation of pistils in WT (C) and *gsd1-D* mutant (G).
(D) and **(H)** SEM observation of anther surface of WT (D) and *gsd1-D* mutant (H).

Figure S3. Comparison of anther development between WT and *gsd1-D* mutant from stage 6 to stage 12 according to established anther developmental stages in rice (Zhang and Wilson, 2009).

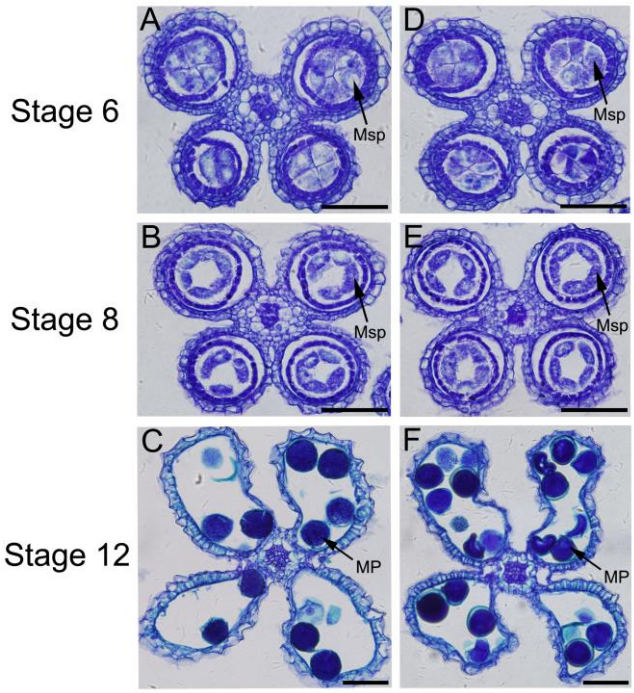

(A-C) Anther development analyzed in WT at stage 6 (A), stage 8 (B) and stage 12 (C). Msp, microspore; MP, mature pollen. Bars = 50 μm.

(D-F) Anther development analyzed in *gsd1-D* mutant at stage 6 (D), stage 8 (E) and stage 12 (F). Msp, microspore; MP, mature pollen. Bars = 50 μm.

Figure S4. I_2-KI staining of starch in the second internode of WT and *gsd1-D* at booting and flowering stages.

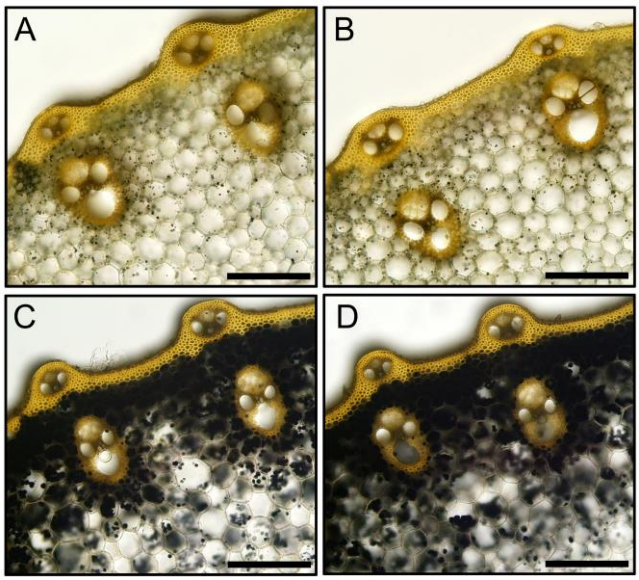

WT (A) and *gsd1-D* (B) starch granules staining at booting stage; WT (C) and *gsd1-D* (D) starch granules staining at flowering stage. Bars = 200 μm.

Figure S5. Expression profiles of the genes involved in starch synthesis between wild-type and *gsd1-D* mutant during rice grain filling.

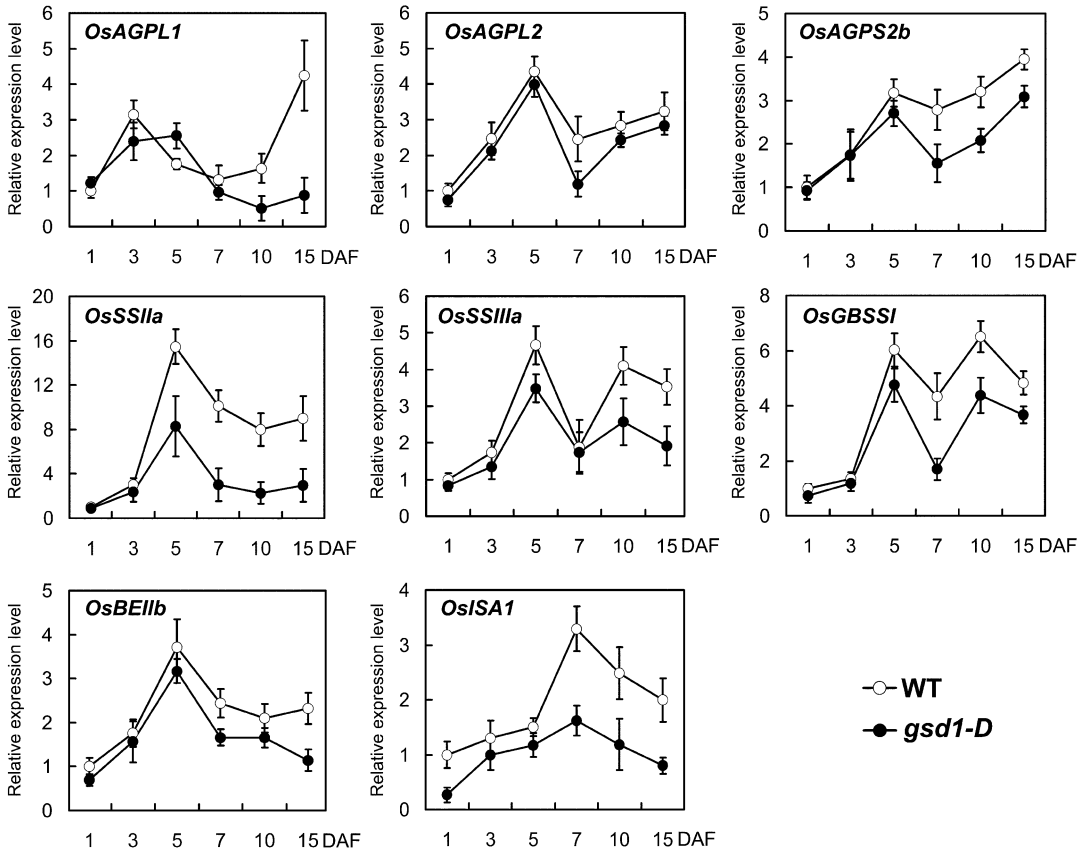

Total RNAs were isolated from 1 to 15 days after flowering (DAF) developing grain of WT and *gsd1-D* mutant. Transcripts of *OsAGPL1, OsAGPL2, OsAGPS2b, OsSS* Ⅱ*a, OsSS*Ⅲ*a, OsBE* Ⅱ*b, OsGBSS* Ⅰ and *OsISA1* were determined using quantitative RT-PCR analysis. Rice *actin1* gene was used as a reference for normalization. Relative gene expression levels in 1 day after flowering (DAF) WT grains were set as 1. The results are means ± SE of independent triplicate assays.

Figure S6. Net photosynthetic activity in flag leaf at 5 DAF in *gsd1-D* mutant and WT plants growing in a greenhouse.

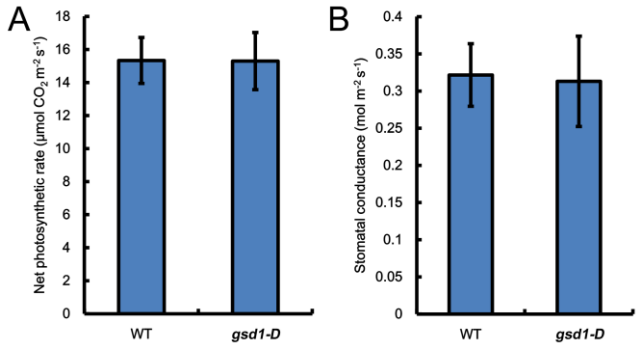

Net photosynthetic rate (P_N) (A) and stomatal conductance (B) were measured using a LI-6400 photosynthesis system (LI-COR). Ten flag leaves from each line were measured. Values are means ± SE.

Figure S7. GC-MS analyses of ^{13}C-labeled soluble sugars in leaf blade and leaf sheath of *gsd1-D* mutant and WT plants.

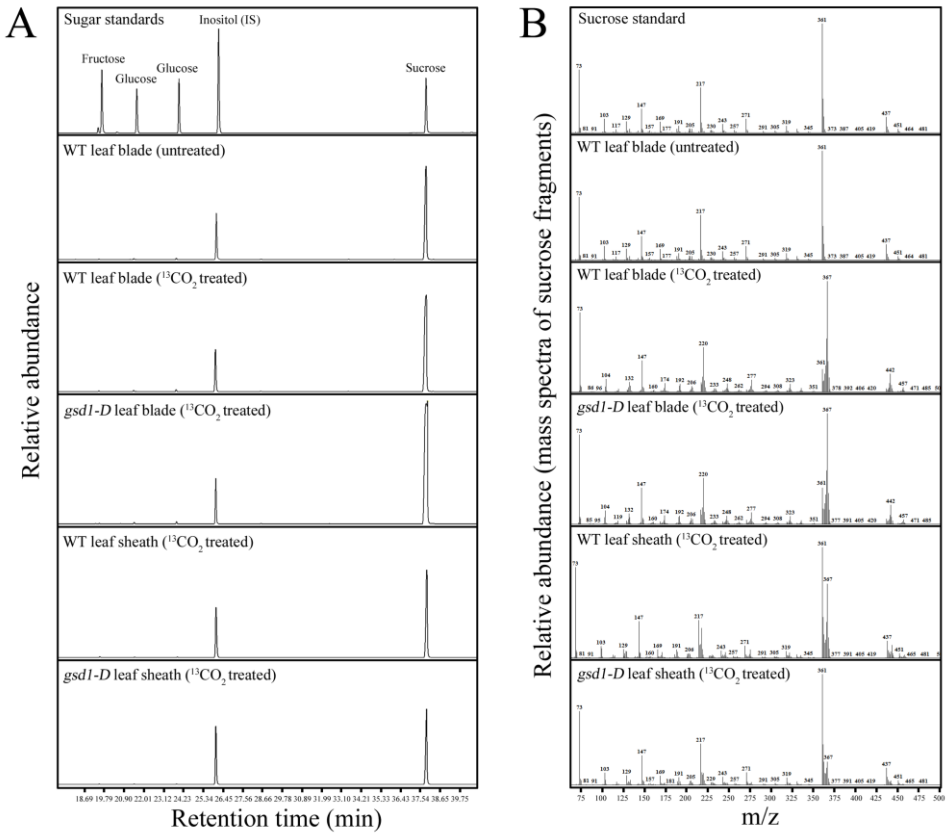

(A) Chromatogram of sugar standards and soluble sugars extracted from rice plants, of which the leaf blade was fed with $^{13}CO_2$ for 12 hr photosynthesis and then kept in dark. The determination was conducted after in dark for 6 hr.

(B) Mass spectrum of the $Si(CH_3)_3$ derivative of sucrose standard and labeled sucrose fragmented in electron ionization (EI) model. The most abundant sucrose fragment is 361, which is shifted to 367 in the ^{13}C-labeled sucrose.

Figure S8. Picture of the chamber used for flag leaf photosynthesis fed with $^{13}CO_2$.

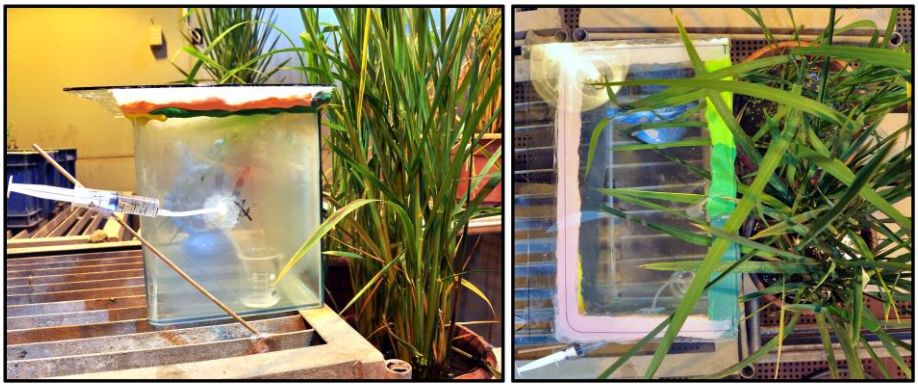

The gas-sealed glass chamber has a lid and a 20 liter space, in which a fan and a thermometer are mounted. A beaker containing sodium bicarbonate-^{13}C is placed in the chamber. ^{13}C-labeling CO_2 is released by addition of 0.5 mM hydrochloric acid through an inlet tube connected with a syringe. The concentration of CO_2 is maintained approximately to 400 ppm through control of hydrochloric acid injection. The chamber was kept in a phytotron and its temperature and photon flux density were maintained as the same as the phytotron regime.

Figure S9. Genotyping analyses of *gsd1-D* T-DNA insertion mutant.

PCR results for genotyping of *gsd1-D* T-DNA insertion lines. F1 and R1 are gene-specific primers, and R2 is the T-DNA specific-primer. W, wild-type; H, heterozygote; M, homozygote.

Figure S10. Amino acid sequences of rice remorins were aligned with the remorins from dicotyledonous Arabidopsis and moss *Physcomitrella patens*.

The remorin family contains 19 members in rice (*Oryza sativa*), 16 members in Arabidopsis (*Arabidopsis thaliana*), and 4 members in moss *Physcomitrella patens*. Remorin protein sequences can be divided in the N-terminal region (underlined with black line) and C-terminal region (underlined with green line). The N-terminal region is highly variable in sequence and in length. The C-terminal region is conserved that contains a coiled-coil domain (shown in red box).

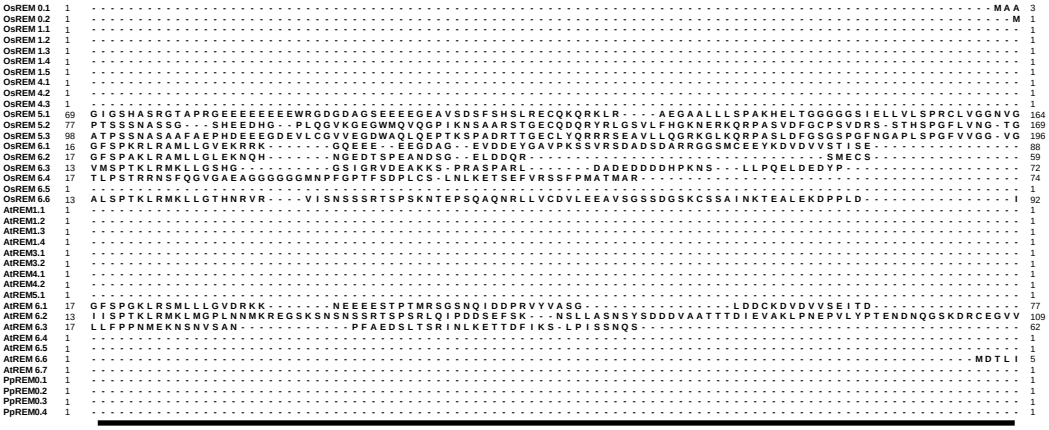

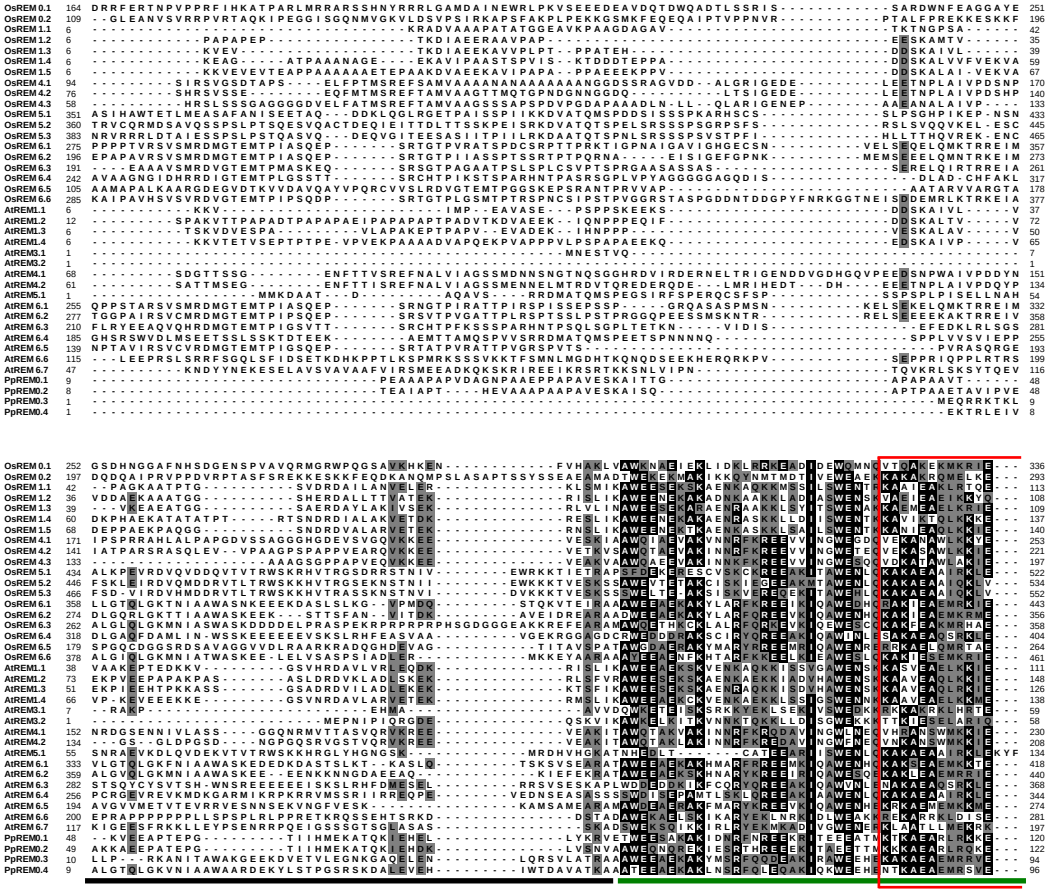
N-terminal residues
C-terminal residues
Coiled-coil domain

Figure S11. Phylogenic analysis and antibody developed for GSD1.

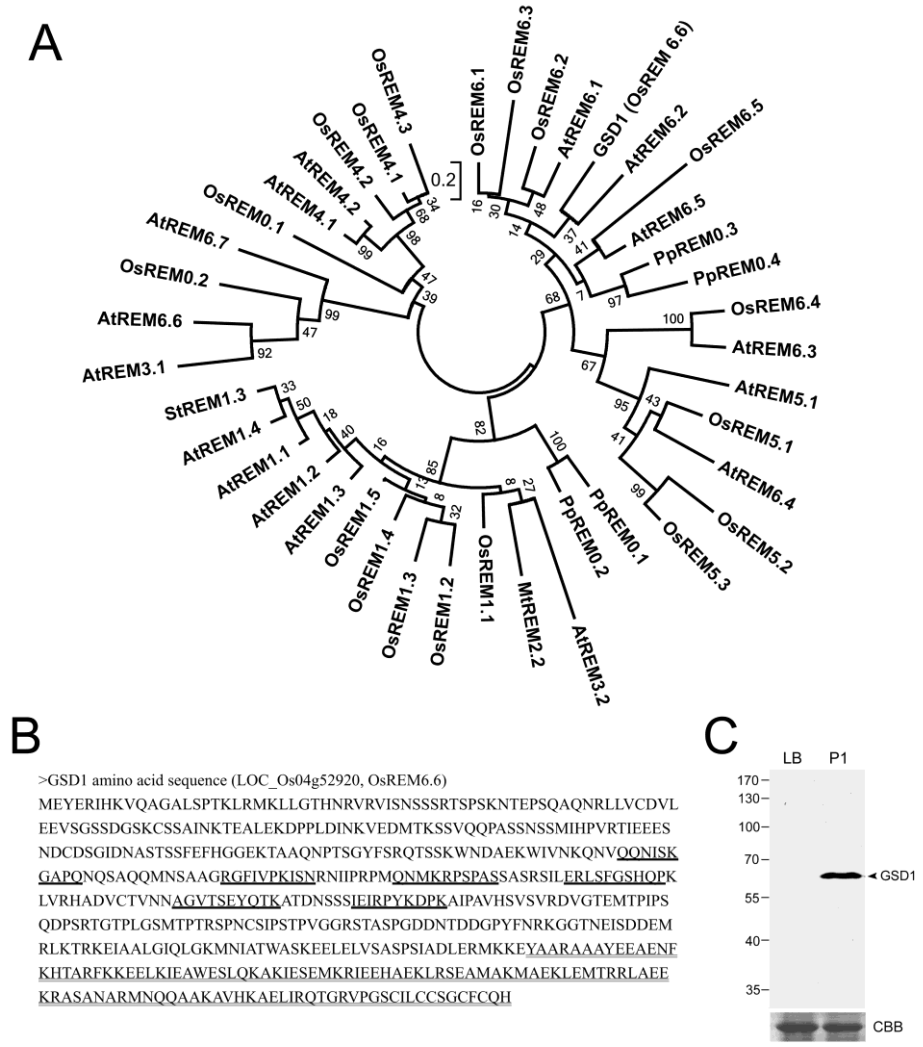

(A) Phylogenetic analysis of GSD1 and its homologs. Unrooted phylogenetic tree of GSD1 and its homologs was constructed with bootstrap values after 1,000 trials using the maximum likelihood method. The scale bar corresponds to 0.2 amino acid substitutions per position in the sequence. Plant species are as follows: *Os, Oryza sativa; At, Arabidopsis thaliana; Pp, Physcomitrella patens; St, Solanum tuberosum; Mt, Medicago truncatula*.

(B and C) *GSD1* specific peptides (peptides of the single underlines) were used to produce polyclonal antibodies (B). The antibody specificity was examined by western blot performed on total extract from leaf blade (LB) and booting panicle (P1) (C). CBB, Coomassie Brilliant Blue.

Figure S12. Phenotypic comparison of wild-type and *GSD1* transgenic plants.

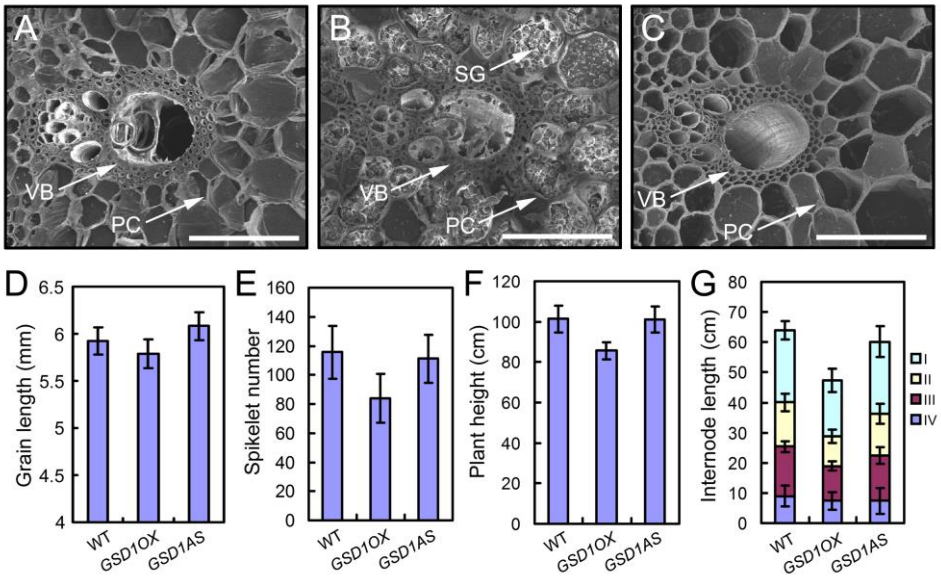

(A-C) SEM observation of the second internode sections of wild-type (E) *GSD1OX* (F) and *GSD1AS* (G) in matured grain plants. PC: parenchyma cell; SG: starch granules; VB: vascular bundle. Bars = 50 μm.

(D-G) Statistic analysis of grain length (D), spikelet number (E), plant height (F), and internode length (G) in WT (left), *GSD1OX* (middle) and *GSD1AS* (right). Sixty seeds were analyzed for seed size. Twenty panicles were analyzed for spikelet number. Twenty plants were analyzed for plant height and internode length. Values are means ± SE.

Figure S13. Net photosynthetic activity in the flag leaves of 5 DAF in WT and GSD1 transgenic plants growing in a greenhouse.

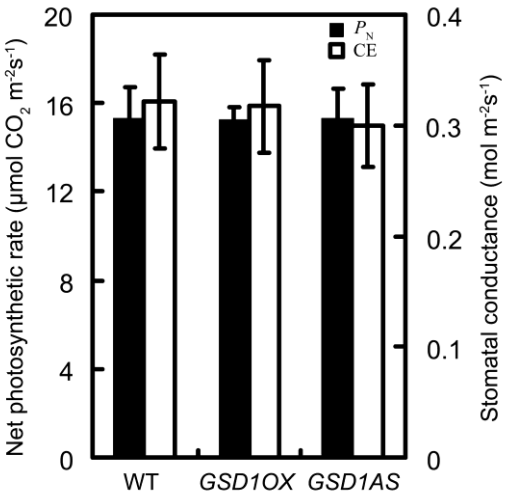

Net photosynthetic rate (P_N) was measured using a LI-6400 photosynthesis system (LI-COR). At least ten flag leaves from each line were measured. Values are means ± SE.

Figure S14. Immunogold labeling of GSD1 in 4 week old rice shoot tissues.

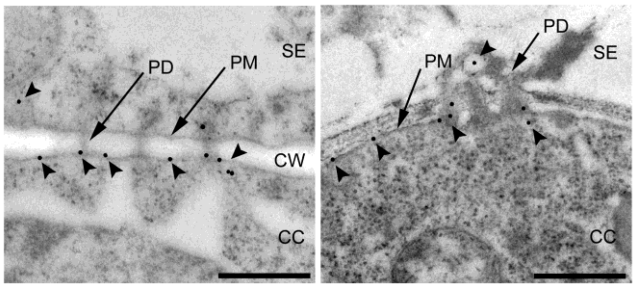

GSD1is localized at the neck regions and the channel of PD and also along the plasma membrane of the companion cells. Arrowheads indicate immunogold labeling particles. CC, companion cell; CW, cell wall; PD, plasmodesma; PM, plasma membrane; SE, sieve element. Bars = 500 µm.

Figure S15. CFDA-based DANS dye loading assays in tobacco (*Nicotiana benthamiana*) leaves.

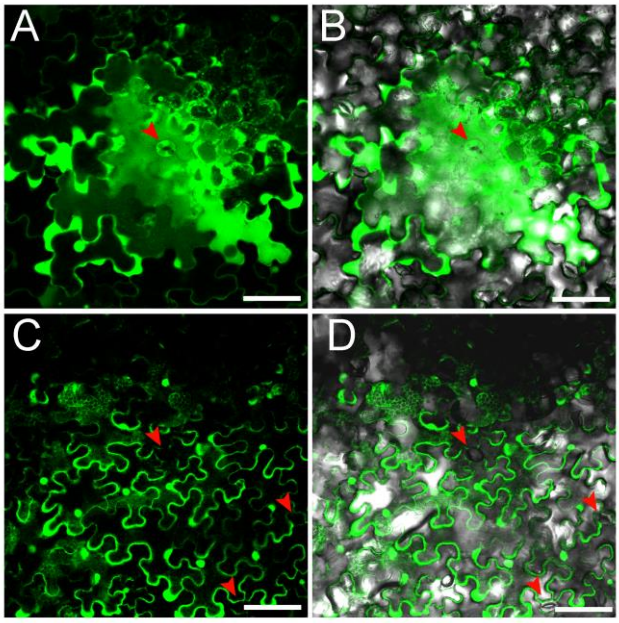

Carboxyfluorescein diacetate (CFDA) was dropped onto the adaxial epidermis of tobacco leaves. CFDA dye entered the pavement cells and guard cells in the adaxial epidermis and was converted by cellular esterase catalysis to CF which illuminates fluorescent signals in the pavement cells and guard cells (A and B). No fluorescent signal is detected in guard cells in the abaxial epidermis (C and D). Red arrowhead indicates mature guard cell. Bars = 100 μm.

Figure S16. Subcellular localization analysis of OsACT1 in tobacco epidermal cells.

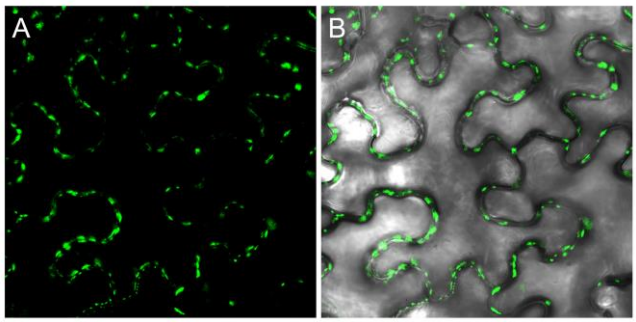

(A) and **(B)** OsACT1 fused to GFP (*GFP-OsACT1*) was transformed into tobacco leaves. Confocal images showing OsACT1 GFP fluorescence signals on PM with spotty distribution (A). OsACT1 GFP fluorescence merged with differential interference contrast (DIC) image (B).

Figure S17. Serial images of z-sections from the top surface to the bottom of the epidermal cells.

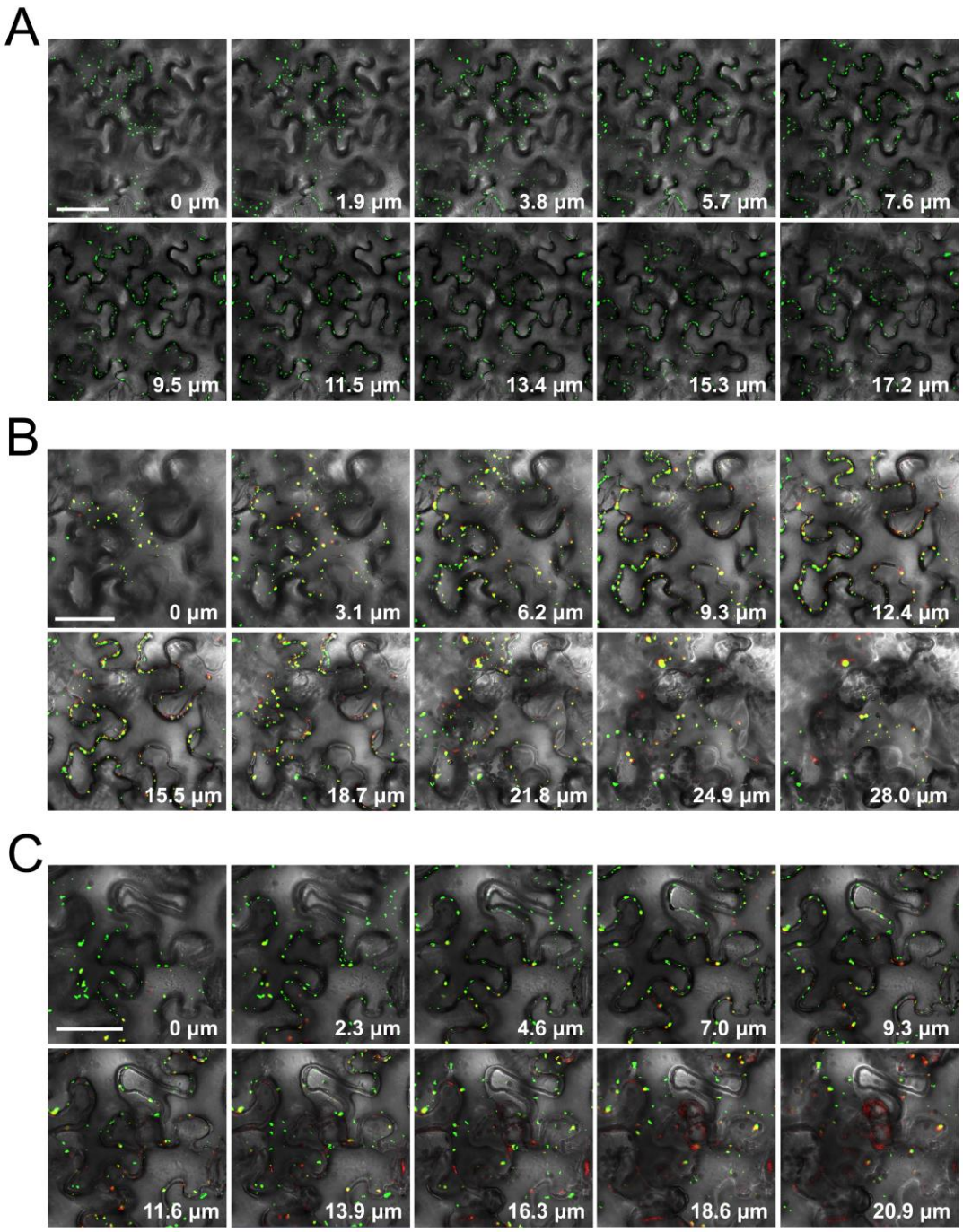

(A) Serial images of z-sections of GFP-OsACT1 fluorescence show that OsACT1 is uneven distributed on the plasma membrane. **(B)** Serial z-section images show that mCherry-GSD1 fluorescence was precisely co-localized with GFP-OsACT1 fluorescence. **(C)** Co-expressed *YN-OsACT1*, *YC-GSD1* and *mCherry-PDCB1* in epidermal cells and the serial z-section images show that mCherry fluorescence was precisely co-localized with YFP fluorescence. Each picture is merged image of fluorescence and DIC channels. Bars = 50 μm.

Supplemental Table 1. Amino acid sequences similarities of rice remorin proteins.

	REM 6.3	REM 6.1	REM 6.2	REM 6.5	REM 6.4	REM 5.1	REM 5.2	REM 5.3	REM 0.2	REM 0.1	REM 1.1	REM 1.2	REM 1.3	REM 1.4	REM 1.5	REM 4.1	EM 4.2	REM 4.3
GSD1 (REM 6.6)	**39**	30	35	21	18	15	15	14	16	**13**	22	24	23	23	24	20	18	21
REM 6.3		34	36	24	20	16	14	15	12	19	26	22	23	20	22	20	19	20
REM 6.1			48	27	20	14	14	14	16	13	27	28	25	23	24	24	21	22
REM 6.2				29	22	19	16	16	14	14	24	26	26	22	22	24	20	20
REM 6.5					21	19	16	18	11	14	18	19	16	17	15	18	17	18
REM 6.4						12	14	14	11	11	18	22	16	16	16	19	14	14
REM 5.1							32	32	12	12	19	18	18	19	19	16	14	16
REM 5.2								52	12	14	18	20	18	13	14	16	16	17
REM 5.3									10	12	16	21	16	15	15	16	16	16
REM 0.2										12	19	18	17	22	20	14	15	14
REM 0.1											19	18	19	18	19	18	18	19
REM 1.1												46	44	51	53	26	23	24
REM 1.2													54	53	54	32	26	26
REM 1.3														49	57	29	28	23
REM 1.4															63	30	24	25
REM 1.5																28	24	22
REM 4.1																	48	39
REM 4.2																		44

Supplemental Table2. List of primers used in this study.

Primer name	Primer sequence (5'→3')	Purpose
GSD1 F	TTCCCCAGTCCCTCCATCT	Cloning
GSD1 R	CGTTGAGCAACAACCAAGTGT	
GSD1P F	GGCTGGAACAAACAAGACAAC	Cloning
GSD1P R	CAATGGGAAATGTCAATTAAGG	
OsACT1 F	ACCACCACCTCCACCTCCTC	Cloning
OsACT1 R	TGAAAACTTTGTCCACGCTAATG	
AtPDLP1 F	AAACAAAAGACAAAAAAAAAACG	Cloning
AtPDLP1 R	AAAAATAAGAATCAATAAGCATCATA	
AtPDLP5 F	AGCAAGTCTTCGCTCTTCAA	Cloning
AtPDLP5 R	TTCCCACTTTGTCCTTTCAT	
AtPDCB1 F	ACATTTTGTCTGAACGCATCT	Cloning
AtPDCB1 R	CTCGAAACGATAACTAAGTGC	
Q-GSD1 F	ACAGAAAAGGTGGCACAAAT	QRT-PCR
Q-GSD1 R	ATGGCTTCGCTTCGCAAT	
OsAct1 F	TCGTCTGCGATAATGGAACT	QRT-PCR
OsAct1 R	CTCGATGGGGTACTTGAGG	
OsAGPL1 F	GGAAGACGGATGATCGAGAAAG	QRT-PCR
OsAGPL1 R	CACATGAGATGCACCAACGA	
OsAGPL2 F	GAGGTTGATGGAAAGATTGAA	These primers were synthesized according to previously reported by Ohdan et al., 2005
OsAGPL2 R	CCTTGTGAGAGGAAAGAGTTG	
OsAGPS2b F	AACAATCGAAGCGCGAGAAA	
OsAGPS2b R	GCCTGTAGTTGGCACCCAGA	
OsSSIIa F	TATGGGGGGAACAGACAG	
OsSSIIa R	GTATCACAAGGACAGAGCGA	
OsSSIIIa F	GCCTGCCCTGGACTACATTG	
OsSSIIIa R	GCAAACATATGTACACGGTTCTGG	
OsBEIIb F	ATGCTAGAGTTTGACCGC	
OsBEIIb R	AGTGTGATGGATCCTGCC	
OsGBSSI F	AACGTGGCTGCTCCTTGAA	
OsGBSSI R	TTGGCAATAAGCCACACACA	
OsISA2 F	TAGAGGTCCTCTTGGAGG	
OsISA2 R	AATCAGCTTCTGAGTCACCG	
pGSD1-L F	TTTTGAATTCACAAGACAACTAC	Promoter-GUS
pGSD1-S F	TTTTGAATTCAGACTAAAAAAGAGG	
pGSD1-LS R	TTTTCCATGGTTCCTCTCTCTC	
F1	CCAAAAGGGGAGTGGTAGC	Genotyping
R1	CCAGTCGCATTTTCTTTCC	
R2	ACAAATCGCCCGCAGAAG	
GSD1OX F	CCGAGCTCCTCCATCTCACTCTC	Overexpression
GSD1OX R	ATATCTAGATCCCTAATTGTCAAGCATACAC	
GSD1AS F	TCTCTAGACCCTCCATCTCACTCTCAC	Anti-sense knockdown
GSD1AS R	TTGAGCTCCCTAATTGTCAAGCATACAC	

L-GSD1 F	AGAGTCTAGAAATGGAGTATGAAAG	Subcellular localization and BiFC
L-GSD1 R	ACAAGATCTTTGACAGAAGCAAC	
L-GSD1N F	AATCTAGACATGGAGTATGAAAGG	Subcellular localization
L-GSD1N R	TTAGATCTTTCTTTCTTCATCCG	
L-GSD1C F	AATCTAGAGAAAGAATATGCAGC	Subcellular localization
L-GSD1C R	TTGGATCCGTGTTGACAGAAG	
L-OsACT1 F	TTAATCTAGATATGGCTGACGCCGAGGATA	Subcellular localization and BiFC
L-OsACT1 R	AATTTGATCATTAGAAGCATTTCCTGTGCA CAAT	
531PDLP1 F	TTTCCTCGAGATGAAACTCACCTATC	Subcellular localization and BiFC
531PDLP1 R	TTTTACTAGTGCATCATATTTATTACTCTTC	
531PDLP5 F	TTTCCTCGAGATGATCAAGACAAAGAC	Overexpression
531PDLP5 R	TTTTACTAGTTTACACCATTTCTCATC	
PDCB1N F	AAAACTCGAGATGGCTGCTCTGGTG	Subcellular localization
PDCB1N R	AAAACCATGGTGAGGCACTAGAATG	
PDCB1C F	AAAATCTAGAGTGTGTGTGTAAGAC	Subcellular localization
PDCB1C R	AAAAGGATCCGAGCATCAGGAAAG	
1007mCherry F	TTTTGTCGACGATGGTGAGCAAGG	Subcellular localization
1007mCherry R	TTTTTCTAGACTTTACTTGTACAGCTCG	
1130mCherry F	TTTTACTAGTGATGGTGAGCAAGG	Subcellular localization
1130mCherry R	TTTTGGATCCTTACTTGTACAGCTC	
2011-YFPN F	TAGTCTCGAGATGGTGAGCAAG	BiFC
2011-YFPN R	AGCTCTAGAGCCATGATATAGACG	
2011-YFPC F	CACTCGAGATGGACAAGCAG	BiFC
2011-YFPC R	TTCTAGAGTCTTGTACAGCTCGTC	

Ohdan T, Francisco PB, Sawada T, Hirose T, Terao T, Satoh H, Nakamura Y (2005) Expression profiling of genes involved in starch synthesis in sink and source organs of rice. Journal of Experimental Botany **56:** 3229-3244